Uncertainties in Interpreting the Scale Effect of Plate Load Tests in Unsaturated Soils

Sai K. Vanapalli and Won Taek Oh

Abstract The applied stress versus surface settlement (*SVS*) behavior from in situ plate load tests (*PLT*s) is valuable information that can be used for the reliable design of shallow foundations (*SF*s). In situ *PLT*s are commonly conducted on the soils that are typically in a state of unsaturated condition. However, in most cases, the influence of matric suction is not taken into account while interpreting the *SVS* behavior of *PLT*s. In addition, the sizes of plates used for load tests are generally smaller in comparison to real sizes of footings used in practice. Therefore, in situ *PLT* results should be interpreted taking account of not only matric suction but also the scale effects. In the present study, discussions associated with the uncertainties in interpreting the *SVS* behavior of *PLT*s taking account of matric suction and scale effects are detailed and discussed.

Keywords Plate load test • Unsaturated soil • Matric suction • Shallow foundation • Bearing capacity • Settlement

1 Introduction

Bearing capacity and settlement are two key parameters required in the design of foundations. There are several techniques available today to determine or estimate both the bearing capacity and settlement behavior of foundations based on experimental methods, in situ tests, and numerical models including finite element analysis. In addition, there are different ground improvement methods to increase the bearing capacity and reduce the settlements. However, in spite of these advancements, various types of damages still can be caused to the superstructures placed on shallow foundations (hereafter referred to as *SF*s) due to the problems

S.K. Vanapalli (✉) • W.T. Oh
Civil Engineering Department, University of Ottawa, Ottawa, ON, Canada
e-mail: vanapall@eng.uottawa.ca; oh.wontaek@gmail.com

S. Chakraborty and G. Bhattacharya (eds.), *Proceedings of the International Symposium on Engineering under Uncertainty: Safety Assessment and Management (ISEUSAM - 2012)*,
DOI 10.1007/978-81-322-0757-3_7,

associated with the settlements leading to cracks, tilts, differential settlements, or displacements. This is particularly true for coarse-grained soils such as sands in which foundation settlements occur quickly after construction. Due to this reason, the settlement behavior is regarded as a governing parameter in the design of *SF*s in coarse-grained soils [25, 26, 34]. Foundation design codes suggest restricting the settlement of *SF*s placed in coarse-grained soils to 25 mm and also limit their differential settlements (e.g., [13]). Such design code guidelines suggest that the rational design of *SF*s can be achieved by estimating the applied stress versus surface settlement (hereafter referred to as *SVS*) behavior of *SF*s reliably instead of estimating the bearing capacity and settlement separately.

The most reliable testing method to estimate the *SVS* behaviors of *SF*s is in situ plate load tests (hereafter referred to as *PLTs)*. In situ *PLT*s are commonly performed on the soils that are typically in a state of unsaturated condition. This is particularly true in arid or semiarid regions where the natural groundwater table is deep. Hence, the stresses associated with the constructed infrastructures such as *SF*s are distributed in the zone above the groundwater table, where the pore water pressures are negative with respect to the atmospheric pressure (i.e., matric suction). Several researchers showed that the *SVS* behaviors from model footings [35, 40, 42, 45] or in situ *PLTs* [16, 39] are significantly influenced by matric suction. However, in most cases, the in situ *PLT* results are interpreted without taking account of the negative pore water pressure above groundwater table. In other words, the influence of capillary stress or matric suction toward the *SVS* behavior is ignored in engineering practice. Moreover, the *PLT*s are generally conducted with small sizes of plates (either steel or concrete) in comparison to the real sizes of foundations. Due to this reason, the scale effect has been a controversial issue in implementing the *PLT* results into the design of *SF*s. These details suggest that the reliability of the design of *SF*s based on the *PLT* results can be improved by taking account of the influence of not only matric suction but also plate size on the *SVS* behaviors.

In this present study, two sets of in situ plate and footing load test results in unsaturated sandy and clayey soils available in the literature are revisited. Based on the results of these studies, an approach is presented such that the uncertainties associated with the scale effects are reduced or eliminated. In addition, discussions on how to interpret the in situ *PLT* results taking account of matric suction are also presented and discussed. Moreover, a methodology to estimate the variation of *SVS* behavior with respect to matric suction using finite element analysis (hereafter referred as *FEA*) is introduced.

2 Plate Load Test

In situ *PLT*s are generally conducted while designing *SF*s [3] or pavement structures [4, 5, 11] to estimate the reliable design parameters (i.e., bearing capacity and displacement) or to confirm the design assumptions. Figure 1 shows typical "applied stress" versus "surface settlement" (*SVS*) behavior from a *PLT*. The peak

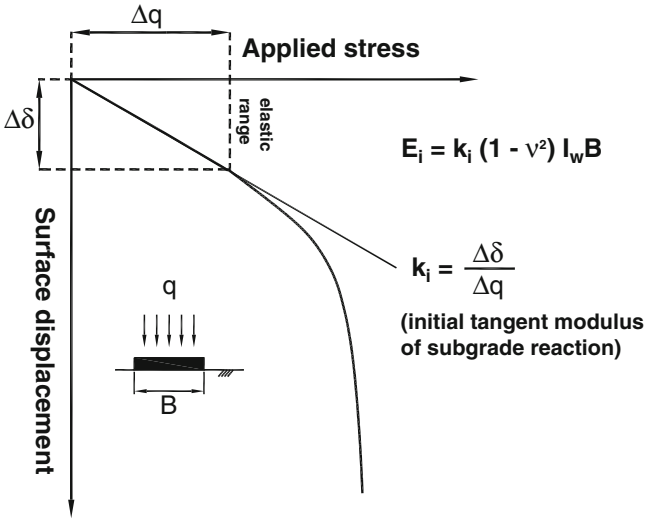

Fig. 1 Typical stress versus displacement behavior from plate load test

stress is defined as ultimate bearing capacity, q_{ult}, for general failure; however, in the case where well-defined failure is not observed (i.e., local or punching failure), the stress corresponding to the 10% of the width of a foundation (ASTM D1194-94) or the stress corresponding to the intersection of elastic and plastic lines of the *SVS* behavior is regarded as q_{ult} [16, 42, 48].

The elastic modulus can be estimated based on the modulus of subgrade reaction, k, that is a slope of *SVS* behavior (i.e., δ versus q) using the theory of elasticity as shown in Eq. (1). The maximum elastic modulus (i.e., initial tangent elastic modulus, E_i) can be computed using the k_i value in the elastic range of *SVS* behavior (initial tangent modulus of subgrade reaction):

$$E = \frac{(1 - v^2)}{(\delta/q)} B I_w = k(1 - v^2) I_w B \tag{1}$$

where E = elastic modulus, v = Poisson's ratio, δ, q = settlement and corresponding stress, B = width (or diameter) of bearing plate, I_w = factor involving the influence of shape and flexibility of loaded area, and k = modulus of subgrade reaction.

Ultimate bearing capacity, q_{ult}, and elastic modulus, E, estimated based on the *SVS* behavior from a *PLT* are representative of soils within a depth zone which is approximately 1.5*B*–2.0*B* [38]. Agarwal and Rana [1] performed model footing tests in sands to study the influence of groundwater table on settlement. The results of the study showed that the settlement behavior of relatively dry sand is similar to that of sand with a groundwater table at a depth of 1.5*B* below the model footing. These results indirectly support that the increment of stress due to the load applied

on the model footing is predominant in the range of 0–1.5*B* below model footing. These observations are also consistent with the modeling studies results by Oh and Vanapalli [31]. This fact also indicates that the *SVS* behavior from *PLT* is influenced by plate (or footing) size since different plate sizes result in different sizes of stress bulbs and mean stresses in soils. This phenomenon which is conventionally defined as "scale effect" needs to be investigated more rigorously to rationally design the shallow foundations.

3 Scale Effect in Plate Load Test

3.1 Scale Effect and Critical State Line

The Terzaghi's bearing capacity factor, N_γ, decreases with an increase in the width of footings [18]. Various attempts have been made by several researchers to understand the causes of scale effects. Three main explanations for the scale effect that generally accepted are as follows:

1. Reduction in the internal friction angle, ϕ', with increasing footing size (i.e., nonlinearity of the Mohr–Coulomb failure envelop) [7, 18, 21]
2. Progressive failure (i.e., different ϕ' along the slip surfaces below a footing) [43, 49]
3. Particle size effect (i.e., the ratio of soil particles to footing size) [41, 43]

According to Hettler and Gudehus [21], there is lack of consistent theory to explain the progressive failure mechanism in the soils below different sizes of footings. In addition, the particle size effect for the in situ plate (or footing) load test (hereafter the term "plate" is used to indicate both steel plate and concrete footing) can be neglected since the ratio of plate size, *B* to d_{50} (i.e., grain size corresponding to 50% finer from the grain size distribution curve), for in situ *PLT*s are mostly greater than 50–100 [24]. The focus of the present study is to better understand the scale effects of *PLT* results and suggest some guidelines of how they can be used in practice.

The reduction in ϕ' with an increasing footing size is attributed to the fact that the larger footing size contributes to a higher mean stress in the soils. In other words, the larger footing induces higher mean stress that contributes to lower ϕ' due to the nonlinearity of the Mohr–Coulomb failure envelop when tested rigorously over a large stress range. This phenomenon can be better explained using the critical state concept ([19]; Fig. 2).

In Fig. 2, the points plotted on the lines *a–b*, *c–d*, and *e–f* simulate the following scenarios:

1. Line *a–b*: Different sizes of footings placed at different depths in sand that have the same initial void ratio value, but the distances to the critical state line are different.

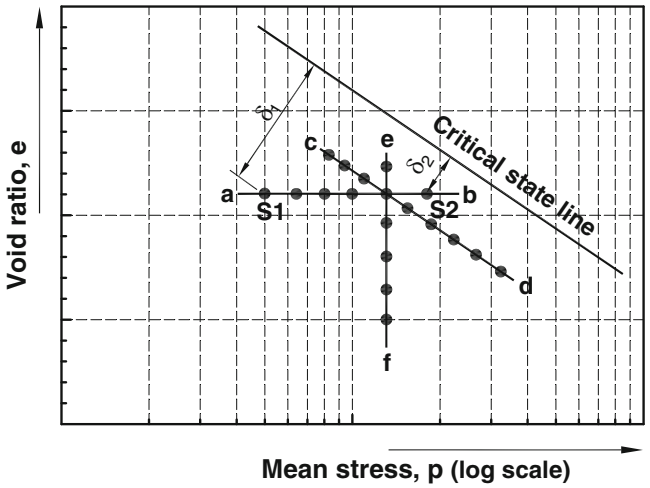

Fig. 2 Relationship between the initial states (i.e., void ratio and mean stress) of soils below footings and critical state line (After Fellenius and Altaee [19])

2. Line *c–d*: Same sizes of footings places at the same depth in sand that have different initial void ratio values, but the distances to the critical state line are the same.
3. Line *e–f*: Different sizes of footings placed at different depths in sands that have different void ratio values, but the distances to the critical state line are the same.

The main concept shown in Fig. 2 is that the behavior of sand below a footing is governed by a distance from the initial state to the critical state line. In other words, the initial states plotted on the line *e–f* will show the same *SVS* behaviors regardless of footing size since the distance to the critical state line for each initial state is the same. On the other hand, the sand below a larger footing (e.g., *S*1 in Fig. 2) will have larger displacement at a certain applied stress in comparison to a smaller footing (e.g., *S*2 in Fig. 2) due to the greater mean stress (i.e., closer to the critical state line) even though the initial void ratio is the same.

3.2 Plate Load Test Results

In this present study, two sets of in situ *PLT*s in sandy and clayey soils available in the literature are revisited to discuss scale effect of *PLT*s.

The Federal Highway Administration (*FHWA*) has encouraged investigators to study the performance of *SF*s by providing research funding. As part of this research project, several series of in situ footing (i.e., 1, 2, 2.5, and 3 m) load tests were conducted on sandy soils. These studies were summarized in a symposium held at the Texas A&M University in 1994 [9] (Fig. 3). Consoli et al. [15]

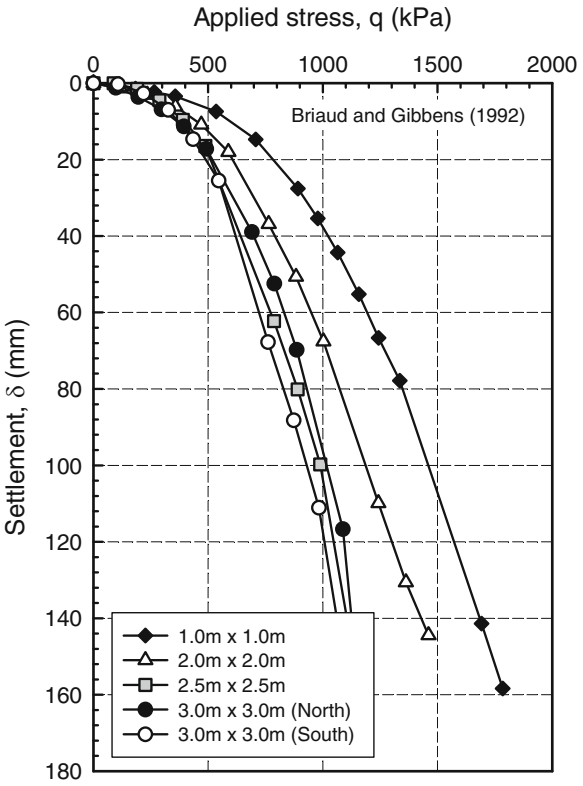

Fig. 3 Stress versus displacement behavior from in situ footing load tests (After Briaud and Gibbens [9])

conducted in situ *PLT*s in unsaturated clayey soils using three steel circular plates (i.e., 0.3, 0.45, and 0.6 m; *PLT*) and three concrete square footings (i.e., 0.4, 0.7, and 1.0 m; *FLT*) (Fig. 4).

As can be seen in Figs. 3 and 4, the bearing capacity increases with decreasing plate size, and different displacement values are observed under different stresses. The *SVS* behaviors clearly show that the *SVS* behavior is dependent of plate size (i.e., scale effect). These observations are consistent with the *SVS* behaviors along the line *a–b* shown in Fig. 2. In other words, the soil below a larger footing induces higher mean stress; therefore, the initial state is closer to the critical state. This phenomenon makes the soil below a larger footing behave as if it is loose soil compared to a smaller footing [12].

3.3 Elimination of Scale Effect of Shallow Foundations

Briaud [8] suggested that scale effect (Fig. 3) can be eliminated by plotting the *SVS* behaviors as "applied stress" versus "settlement/width of footing" (i.e., δ/B) curves

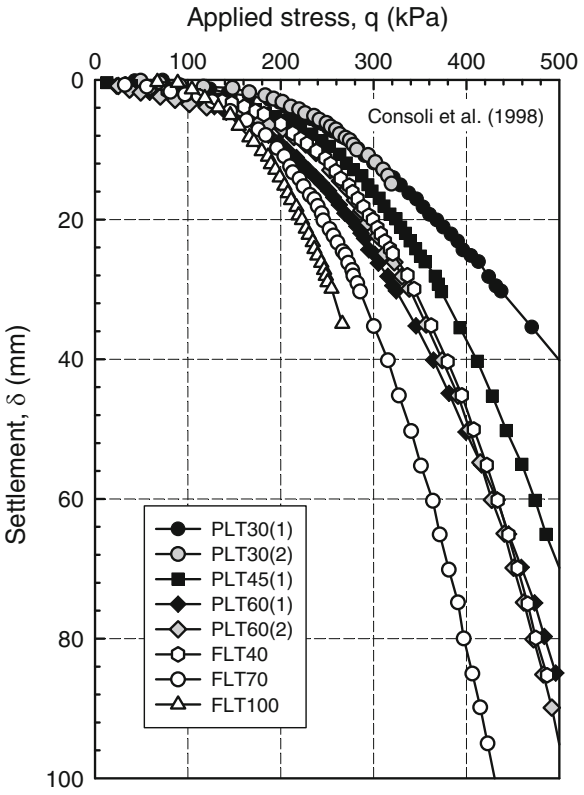

Fig. 4 Stress versus displacement behavior from in situ plate (*PLT*) and footing (*FLT*) load tests (After Consoli et al. [15])

(i.e., normalized settlement; Eq. (2)). Similar trends of results were reported by Osterberg [36] and Palmer [37]:

$$\frac{\delta}{B} = \frac{q(1-v^2)}{E} I_w \tag{2}$$

According to the report published by *FHWA* [10], this behavior can be explained using triaxial test analogy (Fig. 5). If triaxial tests are conducted for identical sand samples under the same confining pressure where the top platens are different sizes of footings, the stress versus strain behaviors for the samples are unique regardless of the diameter of the samples (i.e., the same stress for the same strain). This concept is similar to relationship between q and δ/B from *PLT*s since the term δ/B can be regarded as strain.

Consoli et al. [15] suggested that the scale effect of *PLT*s (Fig. 4) can be eliminated when the applied stress and displacement are normalized with unconfined compressive strength, q_u, and footing width, B, respectively, as shown in Eq. (3). They also analyzed *PLT*s results available in literature [17, 22] and

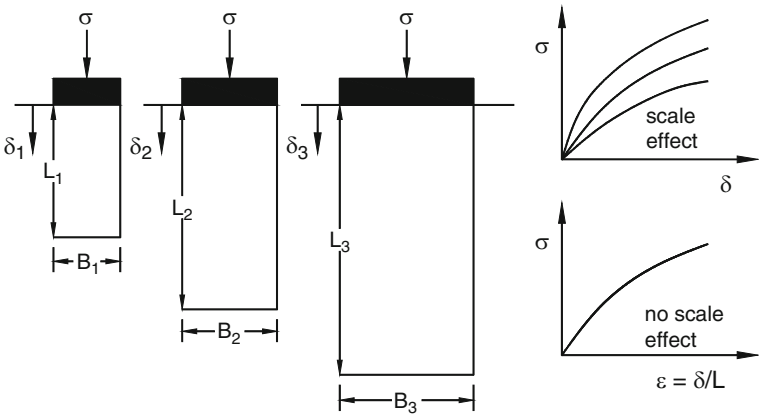

Fig. 5 Triaxial test/shallow foundation analogy [10]

showed that the concept in Eq. (3) can be extended to the *PLT* results in sandy soils as well:

$$\left(\frac{q}{q_u}\right) = \left(\frac{1}{q_u}\right)\left(\frac{E}{1-\nu^2}\right)\left(\frac{1}{C_s}\right)\left(\frac{\delta}{B}\right) = \left\{\frac{C_d}{q_u C_s}\right\}\left(\frac{\delta}{B}\right) \tag{3}$$

where q = applied stress, q_u = unconfined compressive strength at the depth of embedment, δ = surface settlement, B = width of footing, C_s = coefficient involving shape and stiffness of loaded area (I_w in Eq. 1), and C_d = coefficient of deformation ($=E/(1-\nu^2)$).

As can be seen in Figs. 6 and 7, the curves (δ/B versus q) fall in a narrow range. From an engineering practice point of view, these curves can be considered to be unique. Consoli et al. [15] suggested that uniqueness of the normalized curves can be observed at sites where the soils are homogeneous and isotropic in nature.

4 Scale Effect of Plate Size in Unsaturated Soils

The critical state concept discussed above can be effectively used to explain the scale effect of *SF*s in saturated or dry sands. However, this concept may not be applicable to interpret the scale effect of plate size in unsaturated soils since the *SVS* behaviors in unsaturated soils are influenced not only by footing size but also by matric suction value. The influence of matric suction however is typically ignored in conventional engineering practice.

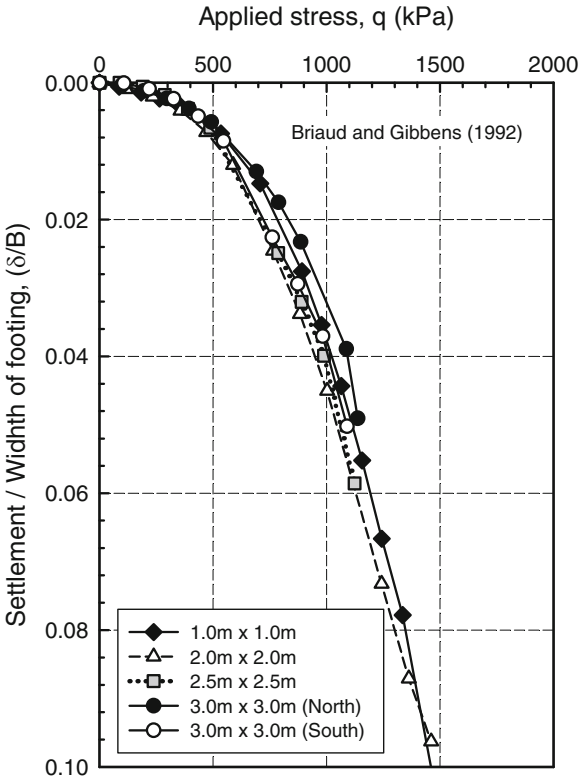

Fig. 6 Normalized in situ footing load test results [9]

4.1 Average Matric Suction Value

Matric suction distribution profile is mostly not uniform with depth in fields. In this case, the concept of "average matric suction" [45] can be used as a representative matric suction value to interpret mechanical properties of a soil at a certain matric suction distribution profile. The average matric suction value, Ψ, is defined as a matric suction value corresponding to the centroid of the suction distribution diagram from 0 to 1.5*B* depth (Fig. 8).

As discussed earlier, the stress increment in a soil due to a load or a stress act on a *SF* is predominant in the range of 0–1.5*B*. Hence, when loads are applied on two different sizes of footings, the sizes of stress bulbs (in the depth zone of 0–1.5*B*) are different (Fig. 9). In other words, the stress bulb for the smaller footing (i.e., B_1) is shallower in comparison to that of the larger footing (i.e., B_2). These facts indicate that the *SVS* behaviors from *PLT*s are governed by *E* and *v* values within the stress bulb. If a matric suction distribution profile is uniform with depth, the average matric suction value is the same regardless of footing size. However, if the matric suction distribution profile is nonuniform, the average matric suction value is dependent on the footing size. For example, the average matric suction value for

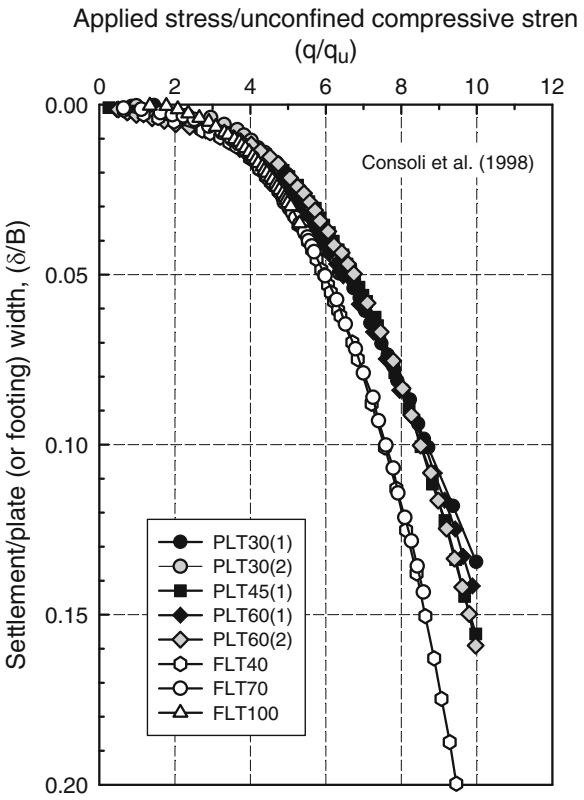

Fig. 7 Normalized in situ plate and footing load test results [15]

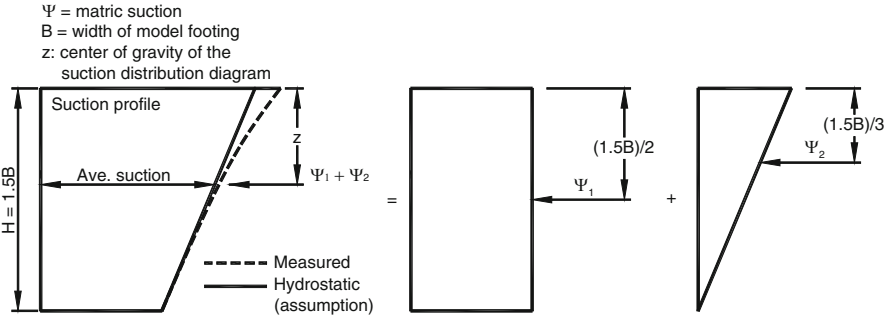

Fig. 8 Estimation of average matric suction value using the centroid of suction distribution diagram

the smaller plate, B_1, (i.e., Ψ_1) is greater than that of larger plate, B_2, (i.e., Ψ_2). In this case, the concept shown in Eqs. (2) and (3) cannot be used to eliminate the scale effect of plate since q_u [29], E_i [34], and v [30, 32, 33] are not constant but vary with respect to matric suction. More discussions are summarized in later sections.

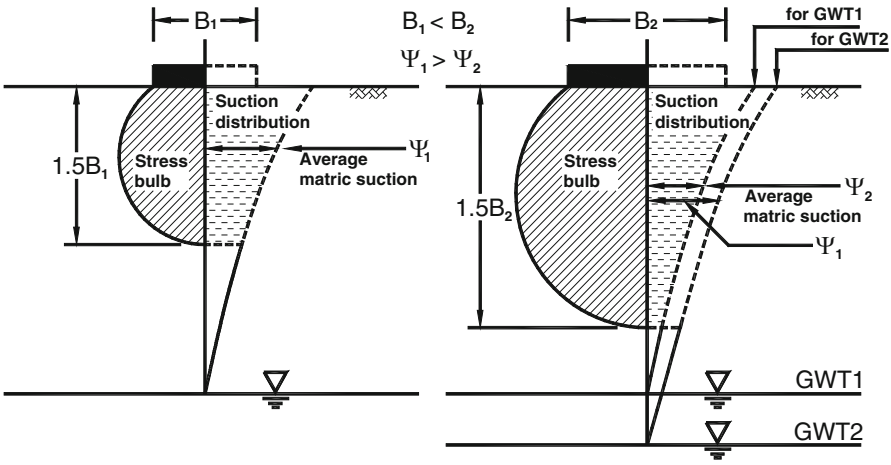

Fig. 9 Average matric suction values for different footing sizes under nonconstant matric suction distribution profile

4.2 *Variation of E_i with Respect to Matric Suction for Coarse-Grained Soils*

Oh et al. [34] analyzed three sets of model footing test results in unsaturated sands [28, 42] and showed that the initial tangent elastic modulus, E_i, is significantly influenced by matric suction. Based on the analyses, they proposed a semiempirical model to estimate the variation of E_i with respect to matric suction using the soil–water characteristic curve (*SWCC*) and the E_i for saturated condition along with two fitting parameters, α and β:

$$E_{i(\text{unsat})} = E_{i(\text{sat})}\left[1 + \alpha \frac{(u_a - u_w)}{(P_a/101.3)}\left(S^{\beta}\right)\right] \tag{4}$$

where $E_{i(\text{sat})}$ and $E_{i(\text{unsat})}$ = initial tangent elastic modulus for saturated and unsaturated conditions, respectively, P_a = atmospheric pressure (i.e., 101.3 kPa), and α, β = fitting parameters.

They suggested that the fitting parameter, $\beta = 1$, is required for coarse-grained soils (i.e., $I_p = 0\%$; *NP*). The fitting parameter, α, is a function of footing size, and the values between 1.5 and 2 were recommended for large sizes of footings in field conditions to reliably estimate E_i (Fig. 10) and elastic settlement (Fig. 11). Vanapalli and Oh [46] analyzed model footing [47], and in situ *PLT* [16, 39] results in unsaturated fine-grained soils and suggested that the fitting parameter, $\beta = 2$, is required for fine-grained soils. The analyses results also showed that the inverse of α (i.e., $1/\alpha$) nonlinearly increases with increasing I_p and the upper and the lower boundary relationship can be used for low and high matric suction values, respectively, at a certain I_p (Fig. 12).

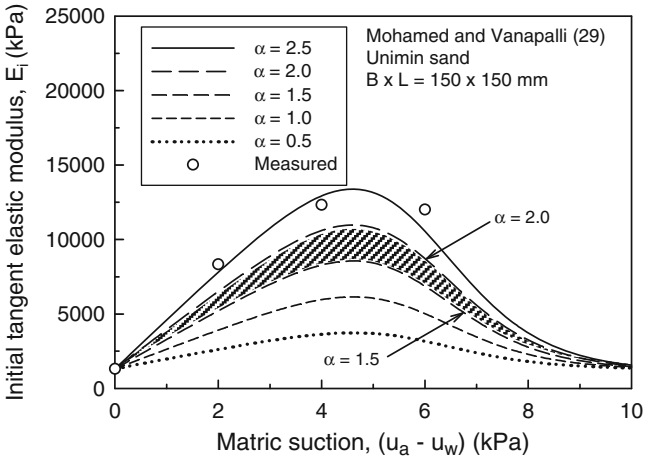

Fig. 10 Variation of modulus of elasticity with the parameter, α, for the 150 mm × 150 mm (Using data from Mohamed and Vanapalli [28])

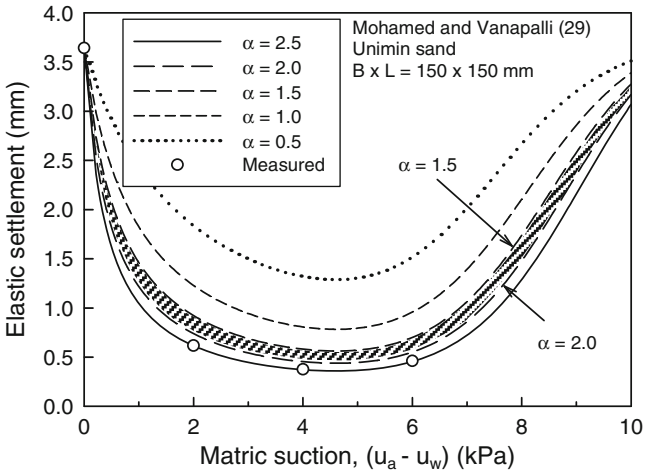

Fig. 11 Variation of elastic settlement with the parameter, α, for the 150 mm × 150 mm footing (Using data from Mohamed and Vanapalli [28])

4.3 Variation of q_u with Respect to Matric Suction for Fine-Grained Soils

Oh and Vanapalli [29] analyzed six sets of unconfined compression test results and showed that the q_u value is a function of matric suction (Figs. 13 and 14). Based on the analyses, they proposed a semiempirical model to estimate the variation of undrained shear strength of unsaturated soils using the *SWCC* and undrained shear

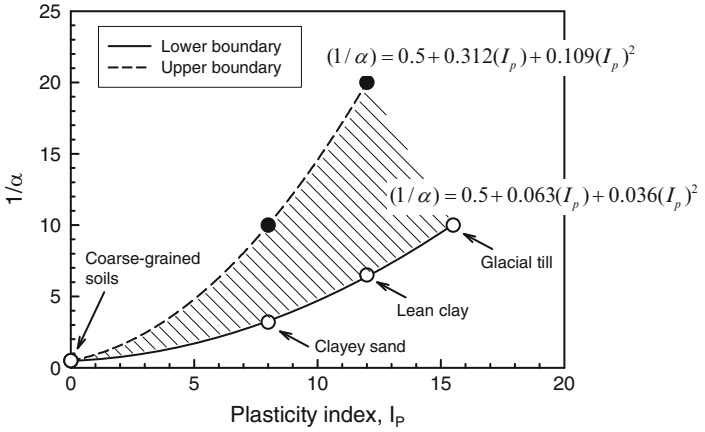

Fig. 12 Relationship between $(1/\alpha)$ and plasticity index, I_p

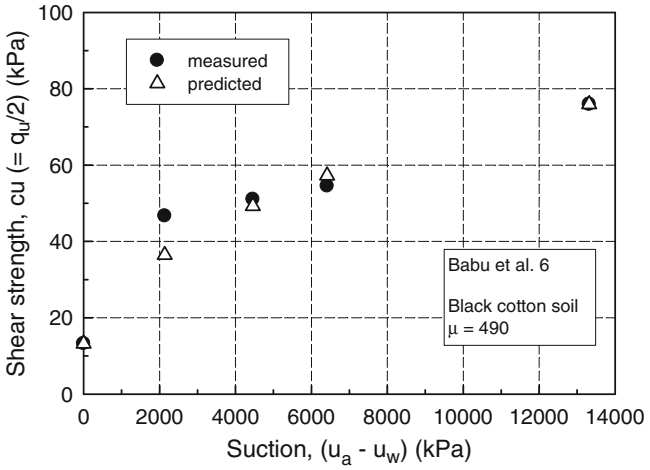

Fig. 13 Comparison between the measured and the estimated shear strength using the data by Babu et al. [6]

strength under saturated condition along with two fitting parameters, v and μ (Eq. 5). Equation (5) is the same in form as Eq. (4):

$$c_{u(unsat)} = c_{u(sat)}\left[1 + \frac{(u_a - u_w)}{(P_a/101.3)}\frac{(S^v)}{\mu}\right] \tag{5}$$

where $c_{u(sat)}$, $c_{u(unsat)}$ = shear strength under saturated and unsaturated condition, respectively, P_a = atmospheric pressure (i.e., 101.3 kPa) and v, μ = fitting parameters.

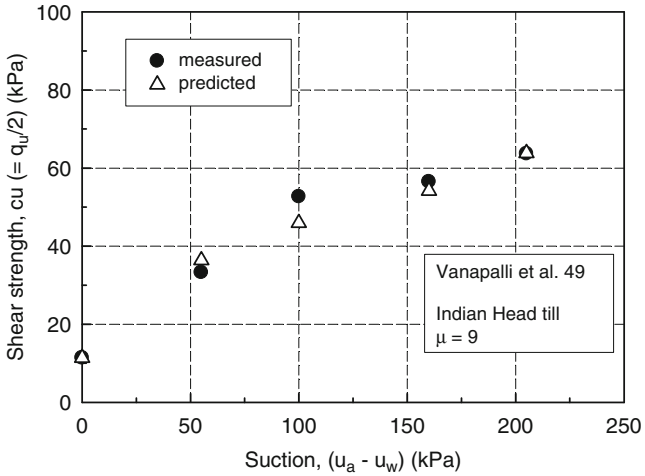

Fig. 14 Comparison between the measured and the estimated shear strength using the data by Vanapalli et al. [47]

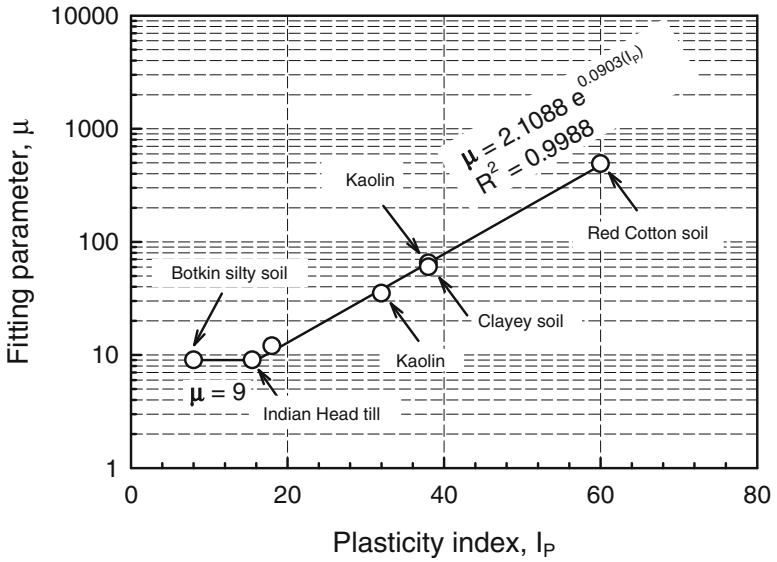

Fig. 15 Relationship between plasticity index, I_p, and the fitting parameter, μ

The fitting parameter, $v = 2$, is required for unsaturated fine-grained soils. Figure 15 shows the relationship between the fitting parameter, μ, and plasticity index, I_p, on semilogarithmic scale for the soils used for the analysis. The fitting parameter, μ, was found to be constant with a value of "9" for the soils that have I_p values in the range of 8 and 15.5%. The value of μ however increases linearly on semilogarithmic scale with increasing I_p.

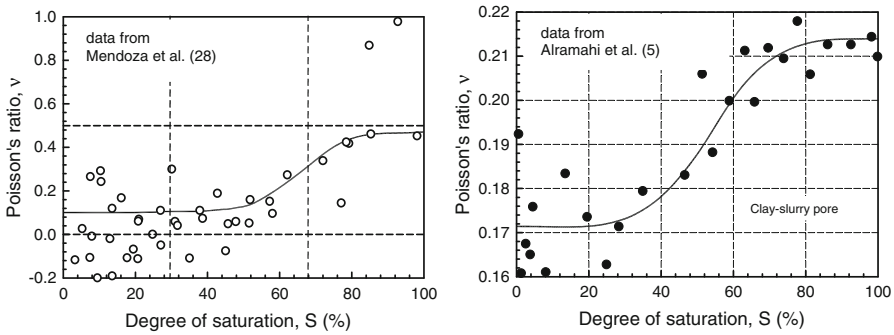

Fig. 16 Variation of Poisson's ratio, v, with respect to degree saturation

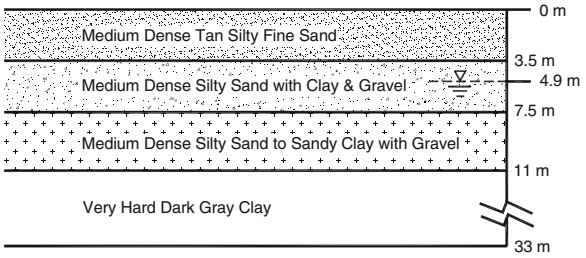

Fig. 17 The average soil profile at the test site (After Briaud and Gibbens [9])

4.4 Variation of v with Respect to Matric Suction

The Poisson's ratio, v, is typically considered to be a constant value in the elastic settlement analysis of soils. This section briefly highlights how v varies with matric suction by revisiting published data from the literature. Mendoza et al. [27] and Alramahi et al. [2] conducted bender element tests to investigate the variation of small-strain elastic and shear modulus with respect to degree of saturation for kaolinite and mixture of glass beads and kaolin clay, respectively. Oh and Vanapalli [33] reanalyzed the results and back calculated the Poisson's ratio, v, with respect to degree of saturation. The analyses of the results show that v is not constant but varies with the degree of saturation as shown in Fig. 16.

5 Reanalysis of Footing Load Test Results in Briaud and Gibbens [9]

The site selected for the in situ footing load tests was predominantly sand (mostly medium dense silty sand) from 0 to 11 m overlain by hard clay layer (Fig. 17). The groundwater table was observed at a depth of 4.9 m, and the soil above the groundwater table was in a state of unsaturated condition. In this case, different

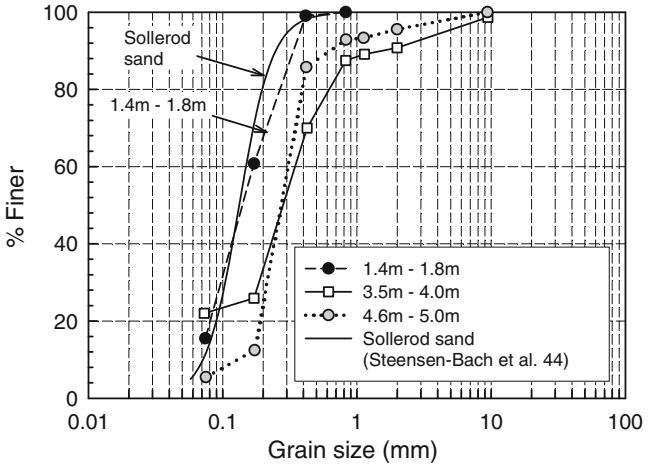

Fig. 18 Grain size distribution curves for the soil samples collected from three different depths [9] and Sollerod sand [42]

Table 1 Summary of the soil properties (From Briaud and Gibbens [9])

Property	Sand (0.6 m)	Sand (3.0 m)
Specific gravity, G_s	2.64	2.66
Water content, w (%)	5.0	5.0
Void ratio, e	0.78	0.75
Effective cohesion, c' (kPa)	0	0
Effective internal friction angle, ϕ' (°)	35.5	34.2

footing sizes may result in different average matric suction values. In other words, scale effect cannot be eliminated with normalized settlement since the soils at the site are not "homogenous and isotropic." Despite this fact, as can be seen in Fig. 6, the *SVS* behaviors from different sizes of footing fall in a narrow range. This behavior can be explained by investigating the variation of matric suction with depth at the site as follows.

Figure 18 shows the grain size distribution curves for the soil samples collected from three different depths (i.e., 1.4–1.8 m, 3.5–4.0 m, and 4.6–5.0 m). The grain size distribution curve the Sollerod sand shown in Fig. 18 is similar to the sand sample collected at the depth of 1.4–1.8 m. The reasons associated with showing the *GSD* curve of Sollerod sand will be discussed later in this chapter. The soil properties used in the analysis are summarized in Table 1.

As shown in Table 1, the water content at the depths of 0.6 and 3.0 m is 5%. This implies that the matric suction value can be assumed to be constant up to the depth of approximately 3.0 m. The field matric suction distribution profile is consistent with the typical matric suction distribution profile above groundwater table for the coarse-grained soils. In other words, matric suction increases gradually (which is close to hydrostatic conditions) up to residual matric suction value and thereafter

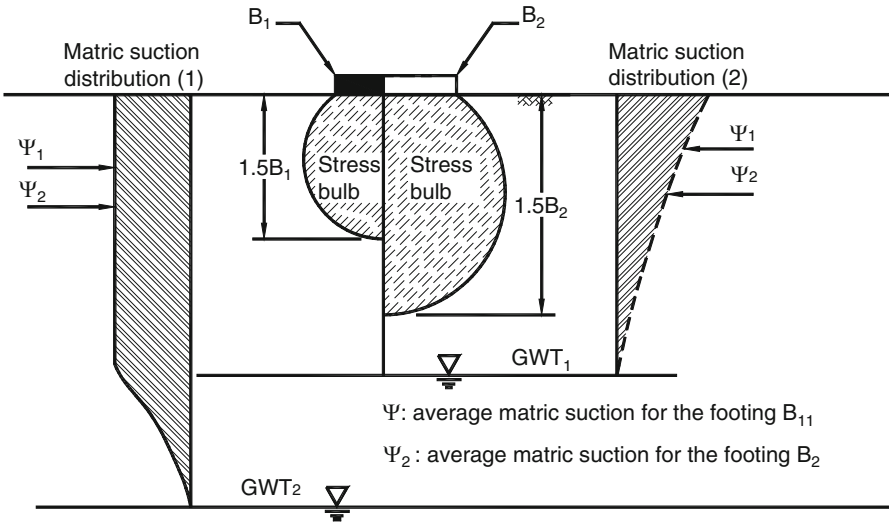

Fig. 19 Average matric suction for different sizes of footing under uniform and nonuniform matric suction distribution

remains close to constant conditions (i.e., matric suction distribution (1) in Fig. 19). This matric suction distribution profile resulted in the same average matric suction value regardless of footing size (for this study). However, it also should be noted that the average matric suction value for each footing can be different if a nonuniform matric suction distribution profile is available below the footings (i.e., matric suction distribution (2) in Fig. 19).

6 Variation of *SVS* Behaviors with Respect to Matric Suction

After construction of *SF*s, the soils below them typically experience wetting–drying cycles due to the reasons mostly associated with the climate (i.e., rain infiltration or evaporation). Hence, it is also important to estimate the variation of *SVS* behaviors with respect to matric suction.

Oh and Vanapalli [32, 33] conducted finite element analysis (*FEA*) using the commercial finite element software SIGMA/W (Geo-Slope 2007; [23]) to simulate *SVS* behavior of in situ footing ($B \times L = 1\text{ m} \times 1\text{ m}$) load test results ([9]; Fig. 3) on unsaturated sandy soils. The *FEA* was performed using elastic–perfectly plastic model [14] extending the approach proposed by Oh and Vanapalli [30]. The square footing was modeled as a circular footing with an equivalent area (i.e., 1.13 m in diameter, axisymmetric problem).

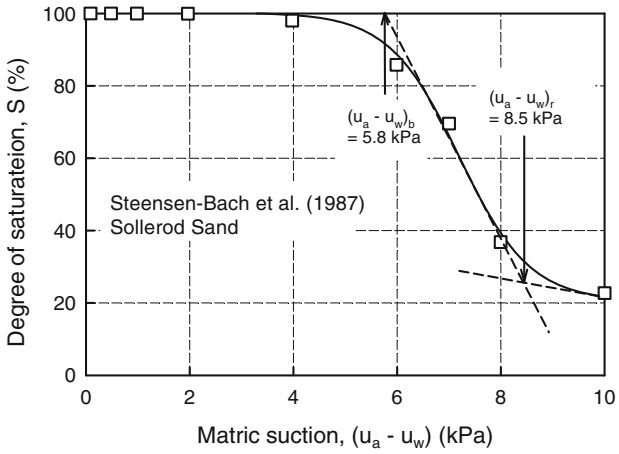

Fig. 20 *SWCC* used for the analysis (Date from Steensen-Bach et al. [42])

The soil–water characteristic curve (*SWCC*) can be used as a tool to estimate the variation of total cohesion, c, (Eq. 6; [44]) and initial tangent elastic modulus, E_i, (Eq. 4) with respect to matric suction:

$$c = c' + (u_a - u_w)(S^{\kappa}) \tan \phi' \tag{6}$$

where c = total cohesion, c' and ϕ' = effective cohesion and internal friction angle for saturated condition, respectively, $(u_a - u_w)$ = matric suction, S = degree of saturation, and κ = fitting parameter ($\kappa = 1$ for sandy soils (i.e. $I_p = 0\%$); [20]).

Information on the *SWCC* was not available in the literature for the site where the in situ footing load test was carried out. Hence, the *SWCC* for the Sollerod sand (Fig. 20) used for the analysis as an alternative based on the following justifications. Among the grain size distribution (hereafter referred as *GSD*) curves shown in Fig. 18, the grain size distribution curve for the range of depth 1.4–1.8 m can be chosen as a representative *GSD* curve since the stress below the footing 1 m × 1 m is predominant in the range of 0–1.5 m (i.e., 1.5*B*) below the footing. This *GSD* curve is similar to that of Sollerod sand (see Fig. 18) used by Steensen-Bach et al. [42] to conduct model footing tests in a sand to understand influence of matric suction on the load carrying capacity. In addition, the shear strength parameters for the Sollerod sand ($c' = 0.8$ kPa and $\phi' = 35.8°$) are also similar to those of the sand where the in situ footing load tests were conducted (see Table 1). The influence of wetting–drying cycles (i.e., hysteresis) and external stresses on the *SWCC* is not taken into account in the analysis due to the limited information.

The variation of *SVS* behavior with respect to matric suction from the *FEA* is shown in Fig. 21. Figure 22a, b shows the variation of settlement under the same stress of 344 kPa and the variation of stress that can cause 25-mm settlement for different matric suction values, respectively. The stress 344 kPa is chosen since the

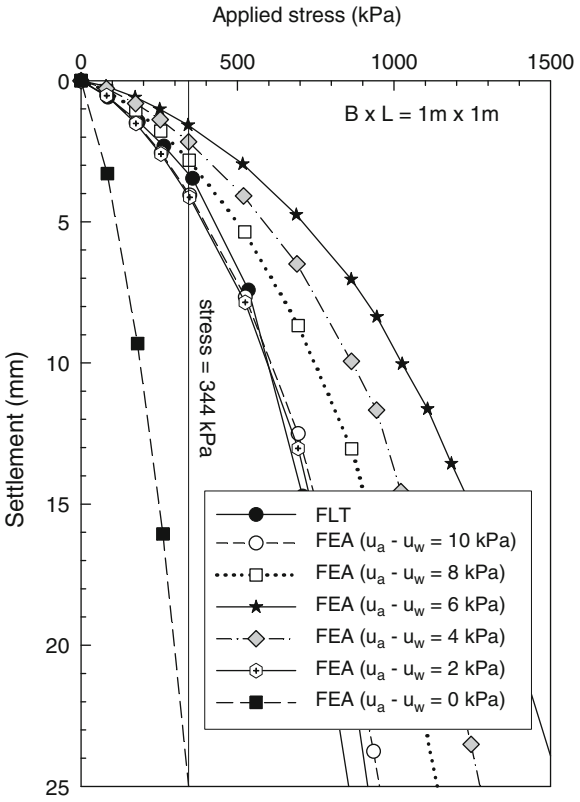

Fig. 21 Variation of *SVS* behavior with respect to matric suction

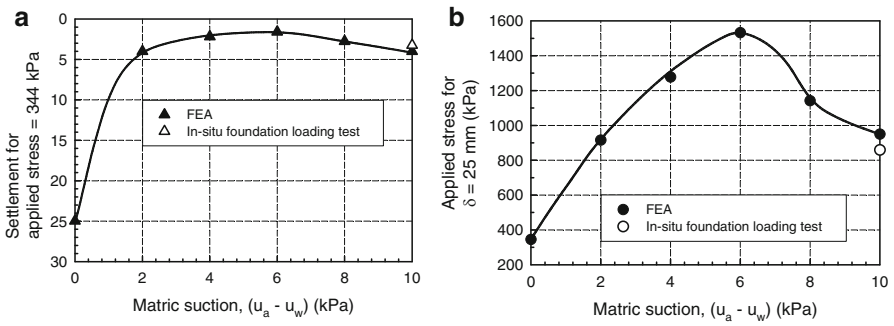

Fig. 22 Variation of (**a**) settlement under the applied stress of 344 kPa and (**b**) stress that can cause 25-mm settlement with respect to matric suction

settlement for saturated condition at this stress is 25 mm. The settlement at the matric suction of 10 kPa (i.e., field condition) is approximately 4 mm and then increases up to 25 mm (i.e., permissible settlement) as the soil approaches saturated conditions under the constant stress (i.e., 344 kPa). The permissible settlement,

25 mm, can be induced at 2.7 times less stress as the soil approaches saturated conditions (i.e., from 10 to 0 kPa). The results imply that settlements can increase due to decrease in matric suction. It is also of interest to note that such a problem can be alleviated if the matric suction of the soil is maintained at 2-kPa value.

7 Summary and Conclusions

Plate load test (*PLT*) is regarded as the most reliable testing method to estimate the applied stress versus surface settlement (*SVS*) behavior of shallow foundations. However, there are uncertainties in interpreting the *PLT* results for soils that are in a state of unsaturated condition. This is mainly attributed to the fact that the *SVS* behavior from the *PLT*s is significantly influenced by both footing size and the capillary stresses (i.e., matric suction). Previous studies showed that the scale effect can be eliminated by normalizing settlement with footing size. This methodology is applicable to the soils that are homogeneous and isotropic with depth in nature such as saturated or dry soils. In case of unsaturated soils, matric suction distribution profile with depth should be taken into account to judge whether or not this methodology is applicable. This is because if the matric suction distribution profile is nonuniform with depth, different plate sizes lead to different average matric suction values. In other words, the soil below the plates cannot be regarded as homogeneous and isotropic since strength, initial tangent elastic modulus, and the Poisson's ratio are function of matric suction. These facts indicate that the reliable deign of shallow foundations based on the *PLT* results can be obtained only when the results are interpreted taking account of the matric suction distribution profile with depth and influence of average matric suction value on the *SVS* behavior.

In case of the shallow foundations resting on unsaturated sandy soils, it is also important to estimate the variation of *SVS* behavior with respect to matric suction. This can be achieved by conducting finite element analysis using the methodology presented in this chapter. According to the finite element analysis for the in situ footing (1 m $\times$ 1 m) load test results discussed in this chapter [9], unexpected problems associated with settlement are likely due to decrease in matric suction. Such a problem can be alleviated if the matric suction of the soil is maintained at a low of 2 kPa.

References

1. Agarwal KB, Rana MK (1987) Effect of ground water on settlement of footing in sand. In: Proceedings of the 9th European conference on soil mechanics and foundation engineering, Dublin, pp 751–754.
2. Alramahi B, Alshibli KA, Fratta D (2010) Effect of fine particle migration on the small-strain stiffness of unsaturated soils. J Geotech Geoenviron Eng 136(4):620–628

3. ASTM D1194-94 (2003) Standard test method for bearing capacity of soil for static load and spread footings. American Society for Testing Materials, Philadelphia
4. ASTM D1195-93 (2004) Standard test method for repetitive static plate load tests of soils and flexible pavement components, for use in evaluation and design of airport and highway pavements. American Society for Testing Materials, Philadelphia
5. ASTM D1196 – 93 (2004) Standard test method for nonrepetitive static plate load tests of soils and flexible pavement components, for use in evaluation and design of airport and highway pavements. American Society for Testing Materials, Philadelphia
6. Babu GLS, Rao RS, Peter J (2005) Evaluation of shear strength functions based on soil water characteristic curves. J Test Eval 33(6):461–465
7. Bolton MD, Lau CK (1989) Scale effects in the bearing capacity of granular soils. In: Proceedings of the 12th international conference of soil mechanics and foundation engineering, vol 2. Balkema Publishers, Rotterdam, pp 895–898
8. Briaud J-L (2007) Spread footings in sand: load settlement curve approach. J Geotech Geoenviron Eng 133(8):905–920
9. Briaud J-L, Gibbens R (1994) Predicted and measured behavior of five large spread footings on sand. In: Proceedings of a prediction symposium, ASCE, GSP41
10. Briaud JL, Gibbens RM (1997) Large scale load tests and data base of spread footings on sand. Publication no. FHWA-RD-97-068. Federal Highway Administration, Washington, DC
11. BS 1377–9:1990 Methods for test for soils for civil engineering purposes. In-situ tests, British Standards Institution, 31 Aug 1990, 70 pp
12. Cerato AB, Lutenegger AJ (2007) Scale effects of shallow foundation bearing capacity on granular material. J Geotech Geoenviron Eng 133(3):1192–1202
13. CFEM (2006) Canadian foundation engineering manual, 4th edn. Canadian Geotechnical Society, Toronto
14. Chen WF, Zhang H (1991) Structural plasticity: theory, problems, and CAE software. Springer, New York
15. Consoli NC, Schnaid F, Milititsky J (1998) Interpretation of plate load tests on residual soil site. J Geotech Geoenviron Eng 124(9):857–867
16. Costa YD, Cintra JC, Zornberg JC (2003) Influence of matric suction on the results of plate load tests performed on a lateritic soil deposit. Geotech Test J 26(2):219–226
17. D'Appolonia DJ, D'Appolonia E, Brisette RF (1968) Settlement of spread footings on sand. J Soil Mech Found Div ASCE 3:735–760
18. De Beer EE (1965) The scale effect on the phenomenon of progressive rupture in cohesionless soils. In: Proceedings of the 6th international conference on soil mechanics and foundation engineering, vol 2(3–6), pp 13–17
19. Fellenius BH, Altaee A (1994) Stress and settlement of footings in sand. In: Proceedings of the conference on vertical and horizontal deformations of foundations and embankments, ASCE, GSP40, College Station, vol 2, pp 1760–1773
20. Garven E, Vanapalli SK (2006) Evaluation of empirical procedures for predicting the shear strength of unsaturated soils. In: Proceedings of the 4th international conference on unsaturated soils, ASCE, GSP147, Arizona, vol 2, pp 2570–2581
21. Hettler A, Gudehus G (1988) Influence of the foundation width on the bearing capacity factor. Soils Found 28(4):81–92
22. Ismael NF (1985) Allowable pressure from loading tests on Kuwaiti soils. Can Geotech J 22(2):151–157
23. Krahn J (2007) Stress and deformation modelling with SIGMA/W. Goe-slope International Ltd.
24. Kusakabe O (1995) Foundations. In: Taylor RN (ed) Geotechnical centrifuge technology. Blackie Academic & Professional, London, pp 118–167
25. Lee J, Salgado R (2001) Estimation of footing settlement in sand. Int J Geomech 2(1):1–28

26. Maugeri M, Castelli F, Massimino MR, Verona G (1998) Observed and computed settlements of two shallow foundations on sand. J Geotech Geoenviron Eng 124(7):595–605
27. Mendoza CE, Colmenares JE, Merchan VE (2005) Stiffness of an unsaturated compacted clayey soil at very small strains. In: Proceedings of the international symposium on advanced experimental unsaturated soil mechanics, Trento, Italy, pp 199–204
28. Mohamed FMO, Vanapalli SK (2006) Laboratory investigations for the measurement of the bearing capacity of an unsaturated coarse-grained soil. In: Proceedings of the 59th Canadian geotechnical conference, Vancouver
29. Oh WT, Vanapalli SK (2009) A simple method to estimate the bearing capacity of unsaturated fine-grained soils. In: Proceedings of the 62nd Canadian geotechnical conference, Hailfax, Canada, pp 234–241
30. Oh WT, Vanapalli SK (2010) The relationship between the elastic and shear modulus of unsaturated soils. In: Proceedings of the 5th international conference on unsaturated soils, Barcelona, Spain, pp 341–346.
31. Oh WT, Vanapalli SK (2011) Modelling the applied vertical stress and settlement relationship of shallow foundations in saturated and unsaturated sands. Can Geotech J 48(3): 425–438
32. Oh WT, Vanapalli SK (2011) Modelling the stress versus displacement behavior of shallow foundations in unsaturated coarse-grained soils. In: Proceedings of the 5th international symposium on deformation characteristics of geomaterials, Seoul, Korea, pp 821–828
33. Oh WT, Vanapalli SK (2012) Modelling the settlement behaviour of in-situ shallow foundations in unsaturated sands. In: Proceedings of the geo-congress 2012 (Accepted for publication)
34. Oh WT, Vanapalli SK, Puppala AJ (2009) Semi-empirical model for the prediction of modulus of elasticity for unsaturated soils. Can Geotech J 46(8):903–914
35. Oloo SY (1994) A bearing capacity approach to the design of low-volume traffics roads. Ph.D. thesis, University of Saskatchewan, Saskatoon, Canada
36. Osterberg JS (1947) Discussion in symposium on load tests of bearing capacity of soils. ASTM STP 79. ASTM, Philadelphia, pp 128–139
37. Palmer LA (1947) Field loading tests for the evaluation of the wheel load capacities of airport pavements. ASTM STP 79. ASTM, Philadelphia, pp 9–30
38. Poulos HD, Davis EH (1974) Elastic solutions for soil and rock mechanics. Wiley, New York
39. Rojas JC, Salinas LM, Seja C (2007) Plate-load tests on an unsaturated lean clay. Experimental unsaturated soil mechanics, Springer proceedings in physics, vol 112, pp 445–452
40. Schanz T, Lins Y, Vanapalli SK (2010) Bearing capacity of a strip footing on an unsaturated sand. In: Proceedings of the 5th international conference on unsaturated soils, Barcelona, Spain, pp 1195–1220.
41. Steenfelt JS (1977) Scale effect on bearing capacity factor N_γ. In: Proceeding of the 9th international conference of soil mechanics and foundations engineering, vol 1. Balkema Publishers, Rotterdam, pp 749–752
42. Steensen-Bach JO, Foged N, Steenfelt JS (1987) Capillary induced stresses–fact or fiction? In: Proceedings of the 9th European conference on soil mechanics and foundation engineering, Dublin, pp 83–89
43. Tatsuoka F, Okahara M, Tanaka T, Tani K, Morimoto T, Siddiquee MSA (1991) Progressive failure and particle size effect in bearing capacity of a footing on sand, GSP27, vol 2, pp 788–802
44. Vanapalli SK, Fredlund DG, Pufahl DE, Clifton AW (1996) Model for the prediction of shear strength with respect to soil suction. Can Geotech J 33(3):379–392
45. Vanapalli SK, Mohamed FMO (2007) Bearing capacity of model footings in unsaturated soils. In: Proceedings of the experimental unsaturated soil mechanics, Springer proceedings in physics, vol 112, pp 483–493

46. Vanapalli SK, Oh WT (2010) A model for predicting the modulus of elasticity of unsaturated soils using the soil-water characteristic curves. Int J Geotech Eng 4(4):425–433
47. Vanapalli SK, Oh WT, Puppala AJ (2007) Determination of the bearing capacity of unsaturated soils under undrained loading conditions. In: Proceedings of the 60th Canadian geotechnical conference, Ottawa, Canada, pp 1002–1009
48. Xu YF (2004) Fractal approach to unsaturated shear strength. J Geotech Geoenviron Eng 130(3):264–273
49. Yamaguchi H, Kimura T, Fuji N (1976) On the influence of progressive failure on the bearing capacity of shallow foundations in dense sand. Soils Found 16(4):11–22